

Extreme X-ray spectral variability in the Seyfert 2 Galaxy NGC 1365

G. Risaliti^{1,2}, M. Elvis¹, G. Fabbiano¹, A. Baldi¹, A. Zezas¹

grisaliti@cfa.harvard.edu

ABSTRACT

We present multiple *Chandra* and *XMM-Newton* observations of the type 1.8 Seyfert Galaxy NGC 1365, which shows the most dramatic X-ray spectral changes observed so far in an AGN: the source switched from reflection dominated to transmission dominated and back in just 6 weeks. During this time the soft thermal component, arising from a ~ 1 kpc region around the center, remained constant. The reflection component is constant at all timescales, and its high flux relative to the primary component implies the presence of thick gas covering a large fraction of the solid angle. The presence of this gas, and the fast variability time scale, suggest that the Compton-thick to Compton thin change is due to variation in the line-of-sight absorber, rather than to extreme intrinsic emission variability. We discuss a structure of the circumnuclear absorber/reflector which can explain the observed X-ray spectral and temporal properties.

Subject headings: Galaxies: AGN — X-rays: galaxies — Galaxies: individual (NGC 1365)

1. Introduction

According to the Unified Model of Active Galactic Nuclei (AGNs, see review by Urry & Padovani, 1995), an axisymmetric absorber/reflector is present around the central black hole of AGNs, with a size between that of the Broad Emission Line Region (BELR, $\sim 1000 R_S$, Schwarzschild radii, corresponding to $\sim 10^{-2}$ pc for a $10^8 M_\odot$ black hole) and that of the Narrow Emission Line region (tens to hundreds parsecs). The simplest geometrical and physical configuration of such absorber is that of a homogeneous torus (Krolik & Begelman

¹Harvard-Smithsonian Center for Astrophysics, 60 Garden St. Cambridge, MA 02138 USA

²INAF - Osservatorio di Arcetri, L.go E. Fermi 5, Firenze, Italy

1988) beyond the dust sublimation radius ($r_{sub} \sim 1.3L_{UV,46}^{-0.5}$ pc, Barvanis 1987, where $L_{UV,46}$ is the UV luminosity in units of 10^{46} erg s $^{-1}$). However, this view has been recently challenged by several pieces of observational evidence:

(1) Dramatic X-ray absorbing column density changes (factors of >10) over a few years have been seen in several type 2 (narrow permitted line) Seyferts (Risaliti, Elvis & Nicastro 2002), ruling out a homogeneous absorber.

(2) Rapid column density variability, on time scales of hours, requires an X-ray absorber no larger than the BELR. Such changes have been detected in the brightest absorbed Seyfert Galaxy, NGC 4151 ($\sim 10 - 30$ hours, Puccetti et al. 2004) and in the Seyfert 2 Galaxy NGC 4388 (4 hours, Elvis et al. 2004). Assuming that the absorber is made of material moving with Keplerian velocity around the central source, these observations imply that its distance is of the order of that of the broad line clouds, i.e. $\sim 10^3 R_S$, where $R_S = 2GM_{BH}/c^2$ is the Schwarzschild radius.

(3) The reflection components in the X-ray spectra of Compton thin Seyfert Galaxies are systematically stronger than expected from reflection off gas with the same column density measured in absorption. This has been shown convincingly for a few sources in which a detailed measurement of the reflection component has been possible (NGC 1365, Risaliti et al. 2000; NGC 2992, Gilli et al. 2002; NGC 6300, Guainazzi et al. 2003) and in a statistical sense in a sample of ~ 20 bright Seyfert 2s (Risaliti 2002).

NGC 1365 ($z=0.0055$) is a particularly striking example of extreme X-ray variability and highly efficient reflection. It was observed by ASCA in 1995 (Iyomoto et al. 1997) in a reflection-dominated state (Thomson optical depth $\tau > 1$, corresponding to $N_H > 1.5 \times 10^{24}$ cm $^{-2}$) and, three years later, in a Compton-thin state ($N_H \sim 4 \times 10^{23}$ cm $^{-2}$) by BeppoSAX (Risaliti et al. 2000). The 2-10 keV flux of the reflection emission was more than 5% that of the intrinsic spectrum measured by BeppoSAX. This corresponds to a ratio $R=1$ between the normalizations of the reflected and direct components in the PEXRAV reflection model (Magdziarz & Zdziarski 1995) Such a high reflection efficiency can be achieved only if a thick ($N_H > 3 \times 10^{24}$ cm $^{-2}$) reflector covers a large fraction of the solid angle around the central source (Ghisellini, Haardt & Matt 1994).

Similar switching from reflection-dominated to transmission dominated states has now been observed in a handful sources on timescales of a few years (Matt, Guainazzi & Maiolino 2004) and could be due either to extreme variations of the intrinsic luminosity and so of the ionization state of the absorber (as suggested by Matt et al. 2004), or to Compton-thick clouds moving across the line of sight, so changing the line of sight column density¹.

¹It is worth noticing the conceptual difference between “reflection dominated” (which merely refers to the observed spectral shape) and “Compton thick” (which implies a physical interpretation of the observed

Here we present an X-ray observational campaign on NGC 1365, consisting of 3 *XMM-Newton* observations, plus a *Chandra* observation (Obsid 3554) performed just three weeks before the first *XMM-Newton* observation. The observing times are relatively short ($\sim 10 - 20$ ksec), therefore a temporal analysis within single observations is not possible. We will therefore discuss the spectra extracted from the whole observations. Two more, longer (60 ksec), *XMM-Newton* observations were recently performed, as a continuation of our program of monitoring of this source. Detailed spectral analysis of all the *XMM-Newton* observations will be presented in a forthcoming paper (Risaliti et al. 2005, in prep.)

Here we will concentrate on the analysis of the most striking result of our study, i.e. dramatic hard X-ray continuum variations: changes from reflection-dominated to transmission-dominated spectra occurred on times scale shorter than three weeks. During this time, the soft thermal component remained constant in all observations. The high resolution of *Chandra* allowed us to resolve this emitting region, which extends over ~ 1 kpc from the center, while the hard component originates in a region < 200 pc (2 arcsec) diameter².

The observation log of the X-ray observations of NGC 1365 is reported in Table 1 together with basic spectral fitting results (§2).

2. Data Analysis and Results

The spectra presented here have been obtained with CCD detectors: the ACIS-S instrument on board *Chandra*, and the EPIC PN and MOS instruments on board *XMM-Newton*. All observations were performed in full-frame mode. We did not find any significant pile-up. This was expected for *XMM-Newton* (the previous published 2-10 keV flux is $< 10^{11}$ erg s⁻¹ cm⁻², mostly emitted at energies > 3 keV), while for *Chandra* this is a consequence of the extremely faint state of the source (Table 1) at that time.

The data were reduced using the standard procedures, using the CIAO v.3.0 package for the *Chandra* observation and SAS v6.0 for the *XMM-Newton* observations. The spectra were extracted from circular regions of a radius of 2" (*Chandra*) and 30" (both *Chandra* and *XMM-Newton*). The background spectra were extracted from regions close to our source and free from contamination by bright serendipitous sources. The background contribution is negligible for the *Chandra* spectrum of the central 2" radius region (thanks to the small

reflection dominated spectrum as due to Compton thick absorption of the direct component).

²Throughout this paper we adopt $H_0 = 70$ km s⁻¹ Mpc⁻¹ (Spergel et al. 2003).

extraction region), and for the two *XMM-Newton* spectra when the source was caught in a bright state (XMM 1 and XMM 3). In the remaining two spectra (XMM 2, and the *Chandra* spectrum from the 30" radius region) the background contamination is $\sim 10\%$.

The spectra were analyzed using the XSPEC 12.0 package. The spectra of the *XMM-Newton* observations are shown in Fig. 1. A visual inspection of this figure is sufficient to clearly notice the main spectral variation: in the 2-10 keV band the XMM 2 spectrum is an order of magnitude weaker than the XMM 1 and XMM 3 observations and has a prominent iron line with an equivalent width $EW > 1$ keV. The continuum is also significantly flatter than in the XMM 1 and XMM 3 5-10 keV spectra (at lower energies, the XMM 1 and XMM 3 spectra are inverted, due to a photoelectric cut off). These features strongly suggest that during the XMM 2 observation the source was in a reflection-dominated state.

One more interesting aspect is the constancy (within 5%) of the soft emission. This suggests that the soft spectrum is dominated by a component not directly related to the primary AGN emission. This is confirmed by the visual analysis of the *Chandra* spectra of the central 2" region, and of the 30" region: most of the soft emission comes from the extended region between 2" and 30" (corresponding to a sphere of outer radius of ~ 2 kpc).

In order to confirm the results of this visual inspection, we performed a detailed spectral analysis of each observation. The complete report on this work will be presented elsewhere (Risaliti et al. 2005, in prep.). In the following we briefly summarize the results relevant for our interpretation of the continuum variations.

Chandra. The *Chandra* spectrum obtained from the central 2" is unusually flat: the photon index of a simple power law model is $\Gamma = -0.1 \pm 0.1$. A good fit is obtained with a cold reflection model (PEXRAV in XSPEC), plus an iron emission line at 6.4 keV (equivalent width $EW = 200_{-120}^{+150}$ eV). A soft thermal component is not required by the data. The spectrum obtained from the larger 30" radius region can be fitted with the same components, plus thermal emission with $kT \sim 0.8$ keV, with a normalization consistent with that found in all the *XMM-Newton* observations. This implies that a) the hard emission comes from the central region; b) the soft component originates from a larger nuclear region (radius ~ 1 kpc).

XMM 1. The first XMM spectrum, obtained only 3 weeks after the *Chandra* observation, is clearly dominated by the direct emission of the AGN above ~ 3 keV. The best fit model consists of all the components used to fit the *Chandra* spectrum, plus an absorbed power law, completely dominating the emission above a photoelectric cut off at ~ 3 keV ($N_H = 4.8_{-0.2}^{+0.3} \times 10^{23}$ cm $^{-2}$) The best fit parameters for the cold reflection are fully consistent with those found in the *Chandra* observation. The ratio between the normalizations of the reflection component and the power law is $R=1.2$.

XMM 2. The second XMM spectrum was obtained 3 weeks after the first. The spectrum is now back in a reflection-dominated state (Fig. 1). The best fit model consists of two components: a cold reflection emission, and an iron emission line at $E=6.4$ keV, with $EW\sim 1.2$ keV. All the parameters of the cold reflection component are consistent with those found in the previous XMM 1 and *Chandra* spectra.

XMM 3. This spectrum, obtained 5 months after the XMM 2 observation, is dominated by the direct emission from the central source. The best fit model is the same as in XMM 1, with a normalization of the direct component higher by 50%, and an absorbing column density $N_H = 3.4_{-0.2}^{+0.2} \times 10^{23}$ cm⁻². The reflection component is consistent with that of XMM 1 and XMM 2. The ratio between the normalizations of the reflection component and the power law is $R=0.8$.

The fit is significantly improved ($\Delta\chi^2 = 45$) by the addition of a broad (possibly relativistic) iron emission line³, although other models, e.g. partial covering and a second, lower N_H , absorber (as in NGC 4151, Zdziarski et al. 2002) may also fit.

3. Discussion

The spectral analysis of multiple *Chandra* and XMM-Newton observations of NGC 1365 reveals transitions from reflection-dominated to transmission-dominated, on time scales no longer than 3 weeks. This is, by a factor of 30, the shortest time scale observed so far for such extreme X-ray spectral variations (Matt et al. 2003) While we also find a kiloparsec scale diffuse origin for the soft thermal component and the possible presence of a relativistic iron line in the highest statistics observation, we will defer discussing of these issues to where we can also consider two new, longer (~ 60 ksec) *XMM-Newton* observations (Risaliti et al. 2005, in prep.). Here we concentrate on the fast spectral transitions.

The extreme column density variations observed from the *Chandra* and XMM 1 observations, and from XMM 1 and XMM 2 can be due to either: (A) fading of the central source, down to a flux 50 times or more fainter than in the “transmission dominated” observations; (B) increased ionization making the absorber more transparent; (C) column density variability, with the reflection dominated spectra having $N_H > 10^{24}$ cm⁻² along the line of sight,

(A) Fading of the central source. In the intrinsic variability scenario, an almost complete switch-off of the source (down to a flux $< 2\%$ of the intrinsic flux in the XMM 1

³This is an important point in itself, however it does not affect our treatment of the continuum variations, therefore we will not discuss it further here, but in Risaliti et al. (2005).

observation) is needed, in a time shorter than 3 weeks. This can be compared with the typical cooling time of the inner part of the accretion disk⁴. The thermal timescale in a Shakura-Sunyaev (1972) disk is approximately $t_{th} \sim (\alpha \times \Omega_K)^{-1}$ (Frank, King & Raine 2002, Starling et al. 2004), where α is the viscosity parameter ($\alpha < 0.1$ for a realistic model), and Ω_K is the Keplerian angular velocity, $\Omega_K = \sqrt{GM_{BH}/R^3}$. The black hole mass, M_{BH} can be estimated from the K magnitude of the galaxy (K=8.4, Jarrett et al. 2003), through the relation between black hole mass and luminosity in the K band (Marconi & Hunt 2003). We obtain $M_{BH} \sim 1.5 \times 10^8 M_\odot$, and $t_{th} > 30 R_{20}^{3/2}$ days, where R_{20} is the linear dimension of the X-ray source in units of $20 R_S$. Given the uncertain assumptions this result is in marginal agreement with our observational requirement $t < 21$ days. However, this requires an extreme scenario, i.e. the complete switch off of the source right after the XMM 1 observation. We conclude that intrinsic variability due to disk cooling is an unlikely explanation for the observed spectral changes. However, in order to rule it out completely, shorter variations (in a timescale of a few days) should be observed.

(B) Ionization changes. In order to make the cold absorber found in the *Chandra* and XMM 2 observations transparent, an increase of the ionization parameter ξ^5 by at least ~ 3 orders of magnitude would be needed (from $\xi < 1$, as required in order to completely obscure the 1-10 keV emission, to $\xi > 10^3$, as required in order to make the gas transparent. This would in turn imply a similar increase in the intrinsic luminosity, which is not seen.

(C) N_H variability. We assume (as in Risaliti et al. 2002, Elvis et al. 2004) that the absorber is made up of gas clouds moving around the central source with Keplerian velocity (motions close to Keplerian dominate in the high ionization parts of the BELR in AGNs, Peterson & Wandel 2000). The variability timescale is then given, to a first approximation, by the crossing time for a cloud across the line of sight. Assuming spherical clouds, the distance R of the absorber from the center is (Risaliti et al. 2002): $R \sim 600 t_{100}^2 n_{10}^2 N_{H,24}^{-2} R_S$ where t_{100} is the variability time in units of 100 ksec, n_{10} is the cloud density in units of 10^{10} cm^{-3} and $N_{H,24}$ is the column density of a single cloud in units of 10^{24} cm^{-2} . Assuming that the variations from Compton thick to Compton thin states were due to a single cloud passing along the line of sight, the measured N_H variation, $\Delta(N_H) = 10^{24} \text{ cm}^{-2}$, corresponds to the column density of a single cloud. We further assume the cloud crossing time to be no longer than the time interval between the XMM 1 and XMM 2 observations, $t_{100} \leq 20$. With these numbers we obtain $R \leq 2 \times 10^5 n_{10}^2 R_S$. A further stringent requirement for the absorbing cloud is to be large enough to cover the X-ray source. Using $M_{BH} = 1.5 \times 10^8 M_\odot$

⁴Here we assume that the fading in the X-rays is due to a decrease of the seed photons from the disk which are up-scattered by the coronal hot electrons.

⁵ $\xi = L(2 - 10 \text{ keV})/nR^2$, where n is the number density of the absorbing gas.

(see above), and assuming again a linear dimension of the X-ray source $D \sim 20 R_S$, we obtain $n < 2 \times 10^9 \text{ cm}^{-3}$ and $R \leq 10^4 R_S = 4.5 \times 10^{17} \text{ cm}$. For comparison, the dust sublimation radius (assuming the standard X-ray to bolometric correction of Elvis et al. 1994) is of the order of 10^{17} cm .

The Compton thick - Compton thin variation discussed here is, by a factor ~ 30 , the fastest observed so far (Matt et al. 2003, Guainazzi et al. 2004). Therefore, the arguments used to rule out the intrinsic variability scenario are significantly less stringent in the other known cases. As a consequence, it is at present impossible to tell whether the observed extreme variability in NGC 1365 is an unique case or is representative of the other known state-changing sources. However, several general considerations can be made on the occurrence of such variations, which are relevant in modeling the circumnuclear medium of AGN, and in driving further studies:

- Compton thick gas seems to be present in (almost) all X-ray obscured Seyfert Galaxies. In $\sim 40\text{-}50\%$ of the sources it covers the line of sight to the central X-ray source (Risaliti, Maiolino & Salvati 1999). In the other X-ray obscured Seyfert Galaxies bright enough to allow a careful X-ray spectral analysis, the high reflection efficiency suggests the presence of Compton thick gas reflecting the primary emission (see Introduction).
- Even if we ascribe all the known thick-thin transitions to N_H variability, this event is still quite rare: only four objects are known to show such variations (Matt et al. 2003) out of the more than 30 known Compton thick AGNs (Comastri 2004). Recently Guainazzi et al. (2004) found one more example (NGC 4939) in a sample of 11 objects.
- The few indications available on short time scale variations (for example this work, and Elvis et al. 2004) suggest that the absorber is rather compact, at a distance of $10^3 - 10^4 R_S$ from the central source.

This observational evidence can be explained if we assume a stratified structure for the circumnuclear absorber/reflector, with a central planar Compton-thick region and a decreasing average column density at greater angles or distance above the disk (Fig. 2). The gas is clumpy and at the distance of the order of that found in NGC 1365 ($\sim 10^4 R_S$). The average number of clouds along a given line of sight is $N \sim 5 - 10$ (except, possibly, for the completely Compton thick region), in order to reproduce the observed average N_H variability in bright AGNs (Risaliti et al. 2002). The angles have been chosen in order to reproduce the observed column density distribution of Risaliti et al. (1999), with fractions of 45%, 25% and 10% of the solid angle covered by gas with column density $N_H > 10^{24} \text{ cm}^{-2}$, $N_H \sim 10^{23} - 10^{24} \text{ cm}^{-2}$, and $N_H \sim 10^{22} - 10^{23} \text{ cm}^{-2}$, respectively, and with the remaining 20% free from absorption, in agreement with the obscured/unobscured Seyferts ratio of Maiolino & Rieke (1995).

In this scheme strong absorption variations are unlikely in the extreme cases of heavily

Compton-thick sources (line of sight through the central region of the absorber) and low obscuration ($N_H = 10^{22} - 10^{23} \text{ cm}^{-2}$) sources (line of sight far from the absorber), while they can happen if the line of sight intersects the transition region between the Compton thick and Compton thin zones. In this simple scheme, NGC 1365 is one of the sources seen through this “transition region”. We note that a similar stratified and compact structure has been proposed to explain the relative X-ray/mid IR absorption properties of Luminous Infrared Galaxies (Risaliti et al. 2000), and to explain the N_H distribution and the megamaser emission in AGNs (Kartje, Königl & Elitzur 1999). In this latter case the distribution arises as the result of a disk wind.

The proposed scheme needs to be tested with more detailed studies of the single sources showing the most extreme variability (a new *XMM-Newton* observational campaign is on going) and with an unbiased statistical analysis of the occurrence of such extreme variations.

We are grateful to A. Siemiginowska and G. Matt for useful discussions. This work was partially supported by NASA grants NAG5-13161, NNG04GF97G, and NAG5-16932.

REFERENCES

- Comastri, A. 2004, in “Supermassive Black Holes in the Distant Universe”, ed. A. J. Barger, (Boston: Kluwer Academic Publishers), 308, 245-172
- Elvis, M., Risaliti, G., Nicastro, F., Miller, J., & Puccetti, S. 2004, *ApJ*, 635, L25
- Frank, J., King, A., & Raine, D. J. 2002, *Accretion Power in Astrophysics: Third Edition*, by Juhan Frank, Andrew King, and Derek J. Raine. Cambridge University Press, 2002
- Ghisellini, G., Haardt, F., & Matt, G. 1994, *MNRAS*, 267, 743
- Gilli, R., Maiolino, R., Marconi, A., Risaliti, G., Dadina, M., Weaver, K. A., & Colbert, E. J. M. 2000, *A&A*, 355, 485
- Guainazzi, M. 2002, *MNRAS*, 329, L13
- Guainazzi, M., Fabian, A. C., Iwasawa, K., Matt, G., & Fiore, F. 2004, *MNRAS*, in press (astro-ph/0409689)
- Iyomoto, N., Makishima, K., Fukazawa, Y., Tashiro, M., & Ishisaki, Y. 1997, *PASJ*, 49, 425
- Jarrett, T. H., Chester, T., Cutri, R., Schneider, S. E., & Huchra, J. P. 2003, *AJ*, 125, 525

- Kartje, J. P., Königl, A., & Elitzur, M. 1999, *ApJ*, 513, 180
- Krolik, J. H. & Begelman, M. C. 1988, *ApJ*, 329, 702
- Magdziarz, P. & Zdziarski, A. A. 1995, *MNRAS*, 273, 837
- Marconi, A. & Hunt, L. K. 2003, *ApJ*, 589, L21
- Matt, G., Guainazzi, M., & Maiolino, R. 2003, *MNRAS*, 342, 422
- Peterson, B. M. & Wandel, A. 2000, *ApJ*, 540, L13
- Puccetti, S., Risaliti, G., Fiore, F., Elvis, M., Nicastro, F., Perola, G.C., Capalbi, M. 2003, Proc. of the BeppoSAX Symposium, The Restless High-Energy Universe, E.P.J. van den Heuvel, J.J.M. in 't Zand, and R.A.M.J. Wijers (Eds), astro-ph/0311446
- Risaliti, G., Maiolino, R., & Salvati, M. 1999, *ApJ*, 522, 157
- Risaliti, G., Maiolino, R., & Bassani, L. 2000, *A&A*, 356, 33
- Risaliti, G. 2002, *A&A*, 386, 379
- Risaliti, G., Elvis, M., & Nicastro, F. 2002, *ApJ*, 571, 234
- Shakura, N. I., & Sunyaev, R. A. 1973, *A&A*, 24, 337
- Spergel, D. N., et al. 2003, *ApJS*, 148, 175
- Starling, R. L. C., Siemiginowska, A., Uttley, P., & Soria, R. 2004, *MNRAS*, 347, 67
- Urry, C. M. & Padovani, P. 1995, *PASP*, 107, 803
- Zdziarski, A. A., Leighly, K. M., Matsuoka, M., Cappi, M., & Mihara, T. 2002, *ApJ*, 573, 505

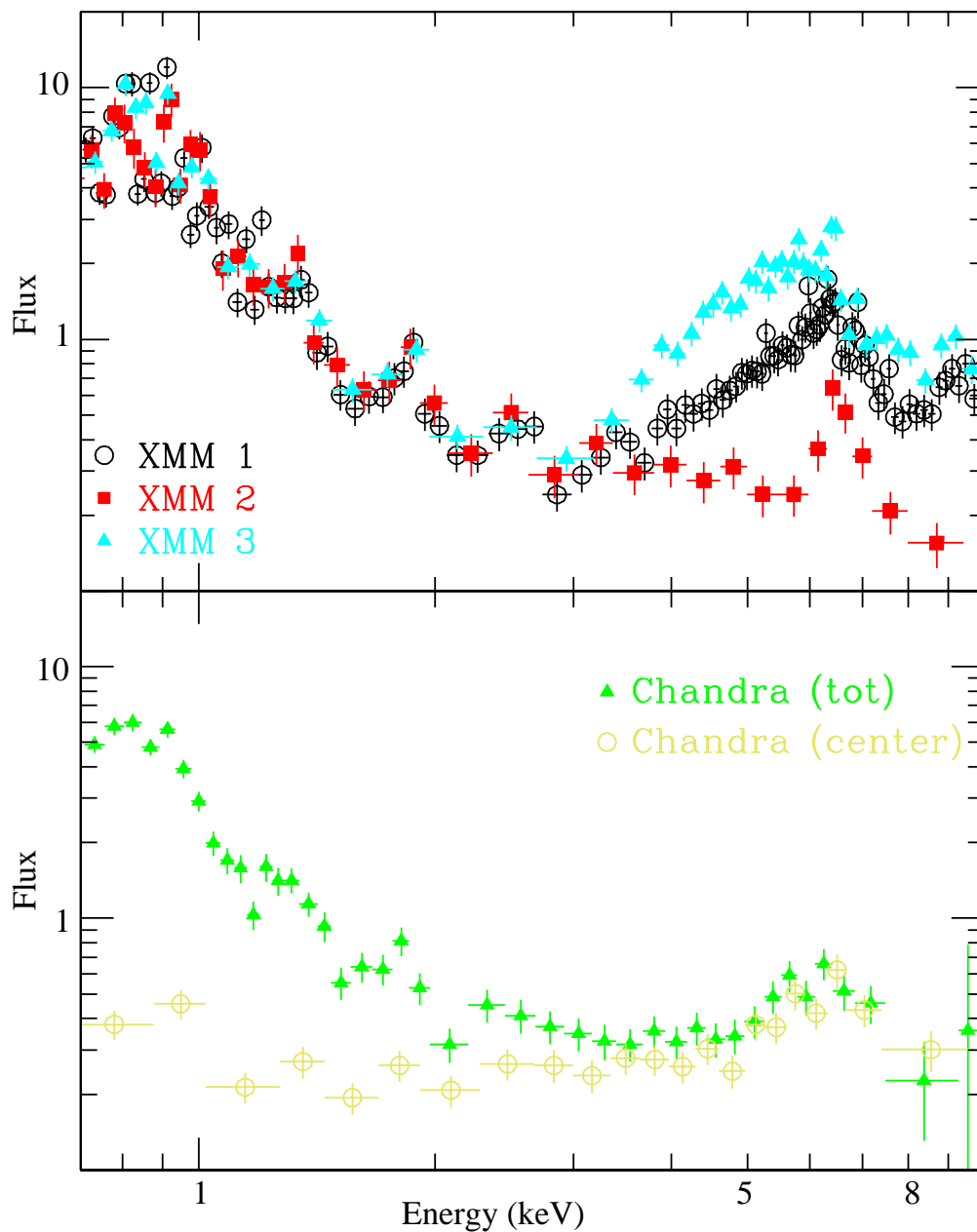


Fig. 1.— Upper panel: Unfolded spectra (using the best fit models of Tab. 1) of the XMM 1, XMM 2 and XMM 3 observations. Central Panel: unfolded spectra of the Chandra observation, extracted from a circular region of 2 arcsec (circles) and of 30 arcsec (triangles), as for the XMM observations. Fluxes are in units of $10^{-4} \text{ erg s}^{-1} \text{ cm}^{-2} \text{ keV}^{-1}$.

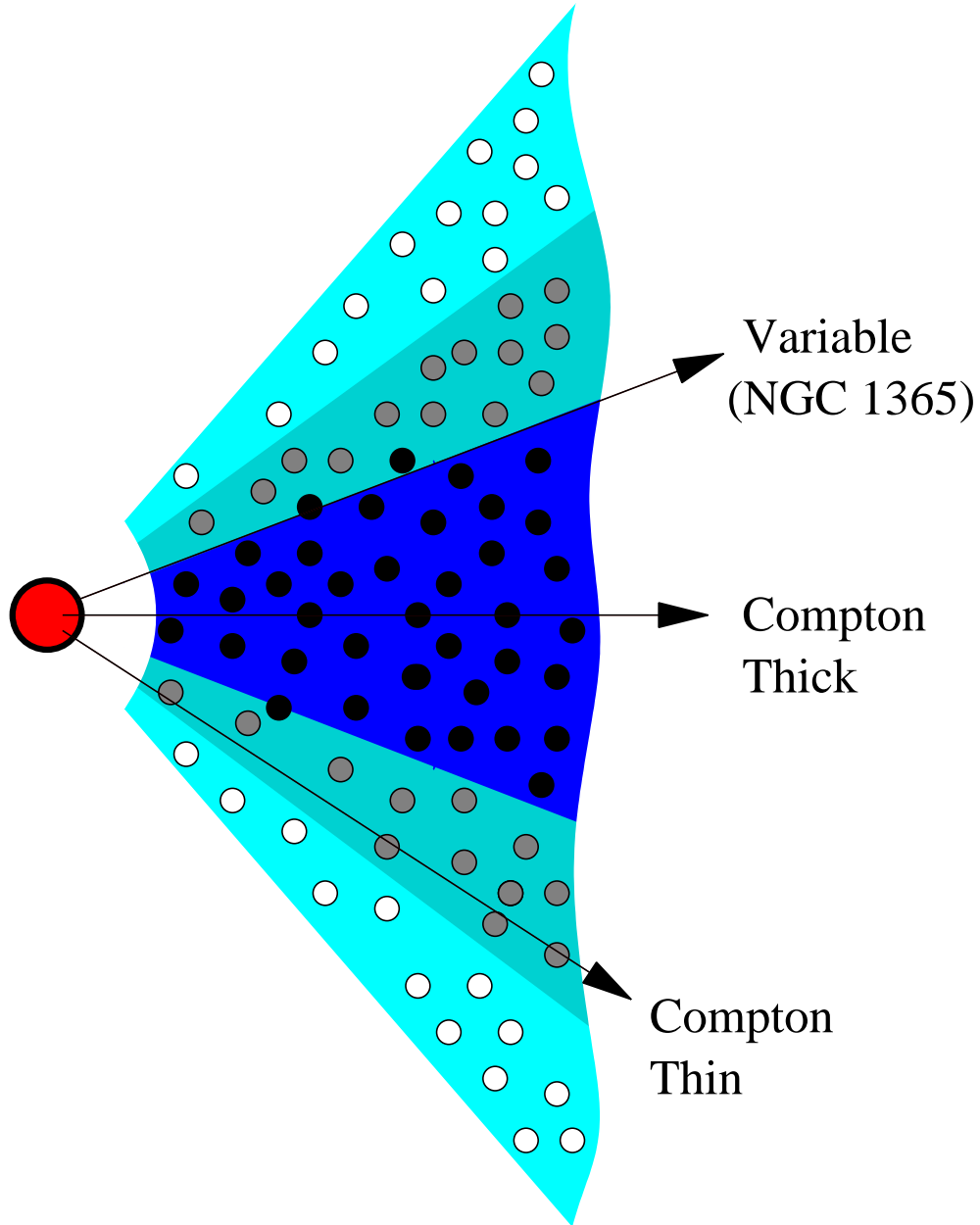


Fig. 2.— Section of the proposed structure of the circumnuclear absorber/reflector. The average column density is indicated by the colors of the background and of the clouds (dark: $N_H > 10^{24} \text{ cm}^{-2}$; medium: $10^{23} \text{ cm}^{-2} < N_H < 10^{24} \text{ cm}^{-2}$; light: $10^{22} \text{ cm}^{-2} < N_H < 10^{23} \text{ cm}^{-2}$). The angles are chosen in order to reproduce the column density distribution of Risaliti et al. (1999).

Table 1: NGC 1365 - X-ray Observation log. & Spectral Fitting Results

Observatory	Date	Counts	T ^a	Γ	N _H ^b	R ^c	F(2-10) ^c	L(2-10) ^d	χ _r ²
<i>Chandra</i> ^f	2002 Dec 24	7478	14.6	1.98 ^{+0.13} _{-0.14} (g)	–	–	0.21	0.14	1.09
XMM-1	2003 Jan 16	14866	17.8	2.06 ^{+0.06} _{-0.03}	47.6 ^{+3.0} _{-1.5}	1.2	0.48	1.23	1.09
XMM-2	2003 Feb 09	3503	5.8	2.09 ^{+0.11} _{-0.14} (g)	–	–	0.17	0.11	1.06
XMM-3	2003 Aug 13	9466	8.7	2.33 ^{+0.12} _{-0.12}	33.5 ^{+1.9} _{-2.0}	0.8	0.70	2.30	1.21

^a: Duration (ksec). ^b: in units of 10²² cm⁻². ^c: Ratio between the normalizations of the reflected and transmitted components. ^d: Observed 2-10 keV flux, in units of 10⁻¹¹ erg s⁻¹ cm⁻². ^e: 2-10 keV luminosity in units of 10⁴² erg s⁻¹. For the transmission dominated spectra, the luminosity is absorption corrected. ^f: 2 arcsec dia. aperture. ^g: photon index of the intrinsic power law in the PEXRAV model.